

Performance of Corrugated Plate Heat Exchanger Using Nano-Fluid

أداء مبادل حراري من النوع ذي الألواح المموجة ومستخدماً نانو سائل

A E Kabeel^{a,1}, T. Abou El maaty^{b,2}, Y.A. F. El-Samadony^{a,3}

^aMechanical Power Department, Faculty of Engineering, Tanta University, Egypt

^bReactors Department, Atomic Energy Authority, Egypt

¹kabeel6@hotmail.com ²talal22969@yahoo.com ³samadony25@yahoo.co.uk

المخلص العربي

لُدفع عملية تحسين خصائص انتقال الحرارة في مبادل حراري من النوع ذي الألواح المموجة تم استخدام نانو سائل. وتعتبر المبادلات الحرارية والتي من النوع ذي الألواح المموجة واحد من أكثر وأوسع أنواع المبادلات استعمالاً. في هذه الدراسة، تم بناء منصة اختبار تجريبي لدراسة الخصائص الحرارية ومعامل انتقال الحرارة والفعالية والقدرة الحرارية المنقولة والانخفاض في الضغط لمبادل حراري من النوع ذي الألواح المموجة ومستخدماً نانو سائل عند تركيزات حجمية مختلفة من أكسيد الألومنيوم (1% - 4%) في الماء النقي. وقد تمت مقارنة النتائج العملية ونتائج النموذج النظري، ولوحظ وجود تقارب بينهما. ولوحظ من النتائج وجود زيادة واضحة في كل من معامل انتقال الحرارة والقدرة المنقلبة بزيادة تركيز مادة النانو. وكانت الزيادة في معامل انتقال الحرارة خلال نظام تدفقي انسيابي في المبادل الحراري تتراوح بين 3.7% - 13%. وذلك عند مجموعة تركيز حجمي لسائل النانو من 1% - 4%. بينما كانت الزيادة المناظرة للانخفاض في الضغط عند نفس الظروف تتراوح بين 4% - 45%.

Abstract— The application of nano-fluids is thought to have a strong potential for enhancing the heat transfer characteristics of the corrugated plate heat exchanger-PHE. The corrugated PHE is one of the most versatile and wide using types of heat exchangers. In this study, an experimental test loop has been constructed to study the PHE thermal characteristics, heat transfer coefficient, effectiveness, transmitted power and pressure drop at different volume fraction of Al₂O₃ nano-material (1% - 4%) in pure liquid water as a base fluid. The experimental results were compared and verified against a theoretical model, a good consistence was noticed. A pronounced increase in both the heat transfer coefficient and the transmitted power was observed by increasing the nano-material concentration. It was found that during laminar flow regime ($Re \leq 2000$) through the PHE, the increase in heat transfer coefficient and in PHE pressure drop is ranging from 3.7% - 13% and 4% - 45% respectively that for a nano-fluid concentration range of 1%vol. - 4% vol.

Key words – Heat transfer, Nano fluid, Nano-material and Plate Heat Exchanger,



1- INTRODUCTION

During the past five decades rapid advances in engineering technology related to nuclear energy, fossil energy, electric power generation, ink-jet printers, and electronic chips cooling have expedited research in a variety of subjects related to heat transfer. Among the subjects, many engineering systems include problems related to heat transfer enhancement in corrugated plate heat exchangers (PHE). Accordingly, various experimental studies for enhancement of the PHE heat transfer have been proposed and studied. In addition to the fundamental nature of the corrugation patterns, these studies incorporated important parameters such as corrugation amplitude, corrugation wave length, corrugation inclination angle and flow rate [6, 7, 14, and 17]. The inclination angle of the crests and furrows of the sinusoidal corrugation heat exchanger pattern relative to the main flow direction has been shown to be the most important design parameter with respect to fluid friction and heat transfer [13]. Modelling and simulation of corrugated PHE have been studied by many authors; a mathematical model is developed in algorithmic form for the steady state simulation of gasket PHE with generalized configurations [19]. With this simulation the temperature profile in all channels, thermal effectiveness, distribution of the overall heat transfer coefficient and pressure drops could be calculated [10,11,19]. The PHE, plate heat exchanger, has a major advantage over the other heat exchangers types, the number of cooling channels can be increased or decreased according to the heat load. Also the PHE performance during the flow degradation is one of the most important subjects that was addressed recently [1].

Nano-fluid technology has emerged as a new technique in recent years. Nano-fluid was

created by Lee et al [12] as a next-generation fluid that may revolutionize heat transfer. By adding tiny particles to a conventional fluid, up to 40% of the fluids capability to transfer heat can be improved. That is, the dispersion solution, (i.e., the nano-fluid), which is produced by dispersing nano-particles into fluids, is known to significantly enhance the poor thermal conductivity of the water [4,12]. The basic phenomenon of nano-fluid is that suspensions that contain solid particles have effective thermal conductivity by their mixing effects. In the past, particles of millimeter or micron scale have been mixed with fluids to improve thermal conductivity; however, all of the studies using that concept have been faced with much problems including sedimentation and clogging due to the large particles size [4, 18, 2, 12, 22 and 23]. The nano-particles used in nano-fluids commonly have a small average size, below 100 nm in diameter Therefore; nano-fluid technology has succeeded in the enhancement of thermal conductivity without the aforementioned problems

I. II. THEORETICAL CONCEPTS

Nano-fluids properties and preparation

Alumina nano-fluids are used in this research because they are widely used in that area of research due to requirements such as stability, homogeneity, and continuous suspension without any outstanding chemical change of the base fluid and also because the physical properties of alumina nano-fluid have been well documented. In this research, the used Alumina nano-particles are manufactured by the patented physical vapour synthesis (PVS) Process of Nanophase Technologies Corporation and have the following physical properties: bulk density = 260 kg/m^3 , true density = 3600 kg/m^3 , specific heat = 765 J/kg K , melting point = $2046 \text{ }^\circ\text{C}$. The properties of the nano-

fluid depend on the properties of the nano-particles, and the surface molecules contributing in the heat transfer mechanism that depends on the size and shape of the particles themselves

The nano-particles used in that study have a shape and dimensions similar to that shown in the photo presented in Figure 1, taken by transmission electron microscopy (TEM), alumina nano-particles have a spherical shape. The size has a normal distribution in a range from 10 nm to 100 nm (47 nm avg. diameter is given from the manufacturer) as shown in Figure 2 [9].

Preparation of nano-particle suspensions is the first step of applying nano-fluids in heat transfer enhancement. In the present study, Al_2O_3 nano-particles were dispersed in distilled water as a base fluid; as a result a new fluid with new physical properties is produced. After measuring the equivalent volume to the required mass of nano-particle powder, four alumina nano-fluids with different mass concentrations for the experiments are prepared by controlling the amounts of the particles. Nano-fluids of 1%, 2%, 3% and 4% volume fraction of particles were prepared. The nano-fluids were treated by ultrasonication without using any dispersant or stabilizer to prevent any possible changes of chemical properties of the nano-fluid due to the presence of additions. The prepared nano-fluids samples were subjected to ultrasonication for about 4 h. No precipitation/settlement of nano-particles was observed after 24 h of settling the suspension. In order to ensure a stable, uniform, continuous suspension, the dispersion solutions are vibrated in an ultrasonic bath for about 8 h just before performing the tests

The solutions were made acidic in order to ensure their stability. The pH value of the

system was adjusted with HCl and NaOH solution by a precise pH Meter (PHS-25, China). The solutions were maintained at a pH of 5.5 to protect the heater surface

Zeta potential is a parameter showing the potential difference between the dispersion medium and the stationary layer of fluid attached to the dispersed particle. The significance of zeta potential is that its value can be related to the stability of colloidal dispersions. So, colloids with high zeta potential (negative or positive) are electrically stabilized, while colloids with low zeta potentials tend to coagulate or flocculate. In general, a value of 25mV (positive or negative) can be taken as the arbitrary value that separates low-charged surfaces from highly charged surfaces. The colloids with zeta potential from 40 to 60 mV are believed to be good stable. For a nanofluid solution with a PH value of 5.5 the absolute Zeta potential is approximately 40 mv. Figure 3 shows the changes of both the zeta potential and the absorbency for Al_2O_3 - and TiO_2 - water nanofluids as a function of pH value [20].

Four alumina nano-fluids with different mass concentrations, the experiments are prepared by controlling the amounts of the particles. The hydrodynamic force acting on the nano-particles surface affected the flow of a liquid-solid solution. So, the volume fraction of the solution is considered a more important factor than the mass fraction, so the following conversion formula is used conventionally, as it is very difficult to measure the precise true volume of nano-particles

$$\phi_v = \frac{1}{\left(\frac{1-\phi_m}{\phi_m}\right) \frac{\rho_p}{\rho_f} + 1} \quad (1)$$

(1)

(1)

(1)

Using the above equation, the next density expression can be used to calculate the two-phase solution density

$$\rho = \rho_f(1 - \phi_v) + \rho_p \phi_v \quad (2)$$

The uncertainty in the nano-fluid calculated density correlation can be approximated to 5% [16].

The specific heat capacity can be measured by using the differential scanning calorimeter (Setaram C80D). The temperature of both the sample and a reference substance is increased with the same rate and the specific heat of the sample is calculated by measuring the difference in heat required to raise the temperature. The uncertainty in the nano-fluid calculated specific can be approximated to 5%, Eq (3) [16].

$$(\rho C_p)_{nf} = (1 - \phi_v)(\rho C_p)_{bf} + \phi_v(\rho C_p)_p \quad (3)$$

Using classical formulas derived for a two-phase mixture and some experimental data [15, 5, 21] the thermal and the physical properties of the nano-fluid under consideration can be computed. All fluid properties are computed at the arithmetic mean between the inlet and the outlet temperature. The rheometer with coaxial cylinders (Haake Rheostress RS600) could be used to calculate the nano-fluid viscosity. The uncertainty in using the nano fluid viscosity correlation is about 5%, [16]

$$\mu_{nf} = \mu_{bf}(123\phi_v^2 + 7.3\phi_v + 1) \quad (4)$$

The thermal conductivity is predicted by the Hamilton - Crosser model, Eq.(5), with less than 5% deviation from the measured value [16]

$$\frac{k_{nf}}{k_{bf}} = \frac{k_p + 2k_{bf} - 2\phi_v(k_{bf} - k_p)}{k_p + 2k_{bf} - \phi_v(k_{bf} - k_p)} \quad (5)$$

Effectiveness - NTU Method

The number of heat transfer unit, NTU method is the one used in the heat exchanger calculation. The effectiveness of the heat exchanger is the ratio of the actual heat transfer rate to the maximum possible heat transfer rate

$$Q = EC_{min}(T_{nf,i} - T_{c,i}) \quad (6)$$

Where Q is the heat transfer from the hot fluid to the cold fluid, E is the heat exchanger effectiveness, C_{min} is the minimum heat capacity rate, $T_{nf,i}$ is the nano-fluid inlet temperature and $T_{c,i}$ is the cooling water inlet temperature.

$$C_{nf} = \dot{M}_{nf} C_{p,nf} \quad (7)$$

$$C_c = \dot{M}_c C_{p,c}$$

For counter flow

$$E_1 = 1 - \exp\left(-NTU\left(1 - \frac{C_{min}}{C_{max}}\right)\right)$$

$$E_2 = 1 - \left(\frac{C_{min}}{C_{max}}\right) \exp\left(-NTU\left(1 - \frac{C_{min}}{C_{max}}\right)\right)$$

$$E = \frac{E_1}{E_2} \quad (8)$$

$$NTU = U.A / C_{min} \quad (9)$$

$$U = 1 / \left(1/h_{nf} + x_{pl}/k_{pl} + 1/h_c\right) \quad (10)$$

$$Re = G \times D_o / \mu \quad (11)$$

$$D_c = 4a \quad (12)$$

$$d = 2a$$

D_e is the equivalent diameter, and a is the amplitude of the sinusoidal corrugation, d is the gap width between two plates and G the coolant mass flux it has the following definitions in both the nanofluid and cooling water sides.

For nanofluid side:

$$G = \dot{M}_{nf} / (N \times d \times w) \quad (13)$$

$$\mu = \mu_{nf} \quad (14)$$

Cooling water-side:

$$G = \dot{M}_c / ((N + 1) \times d \times w) \quad (15)$$

$$\mu = \mu_{bf} \quad (16)$$

Where N is the number of nano-fluid side coolant channels and w is the plate width between gaskets.

III. EXPERIMENTAL APPARATUS AND PROCEDURE

Experimental apparatus

The experimental apparatus given in Fig. 4 was designed in order to carry out the experimental study. The corrugated plate heat exchanger (PHE) is a costly, complicated and a high technique type of heat exchangers. All over the world there are some companies like Alfa - Laval Company have the capabilities to fabricate this type of PHE. A factory of sugar was decommissioning one of its corrugated plate heat exchangers; we have disassembled and cleaned it with some chemicals. A new standard rubber gasket is used during the reassembly. The mini plate heat exchanger (PHE) consists of a pack of corrugated metal plates (6 -plates) form a series of thin channels where the hot and the cold fluids flow and exchange heat through the metal plates, Fig 5. The flow distribution

inside the plate pack is defined by the design of the gaskets, the opened and closed ports of the plates and the location of the feed connections at the covers. The designed configuration of that PHE offered two hot channels and three cold channels. The feed connections are located at opposite sides of the PHE, thus favoring counter current flow between adjacent channels. The plate surface profile was of the corrugated type with a corrugation angle of 30°. Two different water tanks were used to get hot and cold water. Fluids flow rates were measured by rotameter, with a maximum uncertainty of 3%, through a bypass system, two pre-heaters to heat and control the nano-fluid inlet temperature at 40 °C, two centrifugal pumps and two needle valves to provide the required throttling for both the nano-fluid hot loop and the cooling water loop. Six type-k thermocouples with 1.5 mm outer diameter were attached on the corrugated plate surface, three on the hot surface and three on the cold surface of the plate to measure the average surfaces temperatures in both hot and cold sides. The thermocouples used have a maximum precession of 0.1 °C. The inlet and exit temperatures to the PHEs for both the nano-fluid loop and cooling water loop were measured by type-k thermocouples

The PHE pressure drops were measured by a U-tube manometer, one in each loop as shown in Fig.4. Transformer oil with specific gravity of 0.8 is used in the U- Manometer because of its higher sensitivity to low pressure difference than Mercury. Paddle wheel was used to stir constantly the nano-fluid inside the tank during performing the experiments to prevent the chance of any nano-particles deposition or sedimentation inside the tank

This experimental analysis like many other experimental analyses in the same field

experiments were executed out at the laminar flow regime, $Re \leq 2000$

A gradual increase in the average heat transfer coefficient was noticed by increasing the Reynolds number in all experiments. After adding the nano-material, and by increasing the nano-material concentration, the average heat transfer coefficient was increased above the case without nano-material ($\phi = 0.0\%$ vol) due to the enhancement in nano-fluid physical properties especially the nano-fluid thermal conductivity. This enhancement in heat transfer coefficient reached an average percentage of 3.7%, 5.87%, 9.65% and 13% for a nano-material concentration ratio (ϕ) of 1%, 2%, 3% and 4% by volume respectively in the laminar flow regime ($Re \leq 2000$). The obtained experimental results were compared with the theoretical model results described before in section IV, based on [1, 13] and the nano-fluid physical properties (Eq. (1) - Eq. (5)).

Figure 7 shows the PHE experimental results for the effectiveness variation with both Reynolds number and the nano-material concentration. Increasing the Reynolds number is achieved by increasing the amount of the hot fluid hence the total specific heat ratio increases and the number of transfer unit decreases, as shown in Figure 8. The effectiveness decreases as a result of Reynolds number increasing.

When increasing the nano-material concentration above the base fluid case ($\phi = 0.0$), the nano-fluid viscosity increases, hence the Reynolds number decreases, and to fix the Reynolds number values to those in the case with no nano-material, the nano-fluid flow rate must be increased to compensate the reduction in Reynolds caused by the increase in viscosity. As mentioned

before, by increasing the hot nano-fluid flow rate, the PHE effectiveness is decreased due to the increase in the total specific heat ratio and the decrease in the number of transfer unit. So, a high increase in the nano-material concentration causes a high reduction in effectiveness.

Figure 9 shows the experimental results of the PHE transmitted power against the variation in both Reynolds number and the nano-material concentration. The PHE transmitted power increases with increasing Reynolds number due to the enhancement in the heat transfer coefficient, where the heat transfer coefficient is strongly dependent on Reynolds number. When adding a nano-material to the pure liquid water the new nano-fluid thermal conductivity is increased. So, the nano-fluid acquires higher ability for power transmitting than the pure water. Increasing the nano-material concentration increases the amount of power transmitted to the cooling fluid side and a pronounced reduction in hot fluid exit temperature.

The nano-fluid viscosity increases by increasing the nano-material concentration; as a result, the measured pressure drop across the PHE nano-fluid side is increased. The maximum increase in pressure drop recorded was 4% for 1% nano-particle concentration relative to the case without nano-particle. This relative increase was raised to 45%, for 4% nano-particle concentration through the laminar flow measured range ($Re \leq 2000$). It is clear from the results that, the nano-material concentration has a great effect on the pressure drop as shown from Figure 10. The results also showed that; the significant increase in the measured pressure drop, consequently leads to, the necessary pumping power in the case of nano-fluid (4%) is approximately 90% higher than the corresponding value for water due to the

higher kinematic viscosity of the fluid, as shown in Figure 11 and Figure 12. The variation of the pumping power ratio with both Reynolds number and the nano - fluid volume fraction concentration is represented in Figure 12. The pumping power at no nano - fluid state is taken as a reference to those at 1% to 4%. That Figure showed that, required pumping power increase with both the Reynolds number and the nano - particle concentration

V. CONCLUSION

It must be point out that the way the experimental data are presented can lead to different conclusions. In some works, like the current work, the comparison between the nano-fluid and the base fluid results are made on a Reynolds number basis whereas in other works on a velocity basis. Furthermore, for the nano-fluid Reynolds number calculations the properties used are either measured, or estimated using available models and correlations (which are not always accurate.....) and in some cases even the base fluid properties are used, thus making the situation highly ambiguous. In the current work, using the nano-fluid enhances the heat transfer coefficient up to 13 % for a nano-fluid concentration of 4% in laminar flow regime through corrugated plate heat exchanger. The PHE ability for transmitting power is increased as a result of using nano-fluid but the heat exchanger effectiveness was decreased. The pressure drop across the PHE is more sensitive to the increase in nano-fluid concentration. The increase in pressure drop recorded in the range of 4 % - 45% for a nano fluid concentration range of 1%vol. - 4%vol. The experimental work was executed at constant Reynolds number, so the addition of nano-particles to the base fluid introduces higher kinematic viscosity, which requires higher nano-fluid flow to keep

Reynolds number constant; hence the pumping power was significantly increased . It should be indicated that, the increase in nano-fluid thermal conductivity is an essential matter but not enough to achieve high performance in heat exchangers, so further investigations are needed in that field

VI. NOMENCLATURE

A	Total heat transfer area	m^2
a	Amplitude of the sinusoidal	m
C	Fluid total heat capacity	W/K
C _p	Fluid specific heat	J/kg K
D _e	HEX. Channel equivalent	m
d	Gap width between two plates,	m
E	HEX. Effectiveness	
G	Fluid mass flux in channel	$kg/m^2 s$
h	Heat transfer coefficient	$W/m^2 K$
k	Thermal conductivity	W/ m k
L	HEX. Effective plate length	m
M	Fluid flow rate	kg/s
N	Number of nanofluid side cooling	
NTU	Number of heat transfer units	
Q	Heat transfer	W
T	Temperature	K
U	Overall heat transfer coefficient	$W/m^2.k$
w	HEX. Plate width,	m
x	HEX. Plate thickness	m
<i>Greek</i>		
ϕ	particle concentration	
θ	HEX. corrugation inclination	
ρ	Fluid density,	kg/m^3
μ	Fluid viscosity,	$N s/m^2$
<i>Subscripts</i>		
bf	base fluid	
c	cooling water or cold fluid	
ci	cold fluid inlet	
ch	rRelated to channel	
f	fluid	
h	hot fluid	
hi	hot fluid inlet	
m	mass	
min	minimum	
max	maximum	
nf	nanofluid	
p	particle	
pl	HEX .plate	
v	volume	

VI. REFERENCES

1. Abou-Elmaaty, T., Plate heat exchanger – inertia flywheel performance in loss of flow transient, *KERNTECHNIK*, vol. 74, pp. 35-41, 2009.
2. Das, S. K., Putra, N. and Roetzel, W., Pool boiling characteristics of nano-fluids, *Int. J. Heat Mass Transfer* vol. 46, pp. 851–862, 2003.
3. Durumus, A., Investigation of heat transfer and pressure drop in plate heat exchangers having different surface profiles, *International Journal of Heat and Mass Transfer*, vol. 52, pp. 1451 – 1457, 2009. [4]
4. Eastman, J. A., Choi, U.S., Li, W. and Yu, L.J., Thompson, Anomalously increased effective thermal conductivities of ethylene glycol-based nano-fluids containing copper nano-particles, *Appl. Phys. Lett*, vol. 78, no.6, pp. 718–720, 2001.
5. Eastman, J.A., Choi, S.U., Li, S., Soyez, G., Thompson, L. J. and DiMelfi R. J., Novel thermal properties of nano-structured materials. *J. Metastable Nanocryst Mater* vol. 2, no. 6, pp. 629-634, 1999.
6. Focke, W. W., Zachariades, J. and Olivier, I., The effect of corrugation angle on the thermohydraulic performance of plate heat exchangers. *Int. J. Heat Transfer*, vol. 28, pp. 1469–1479, 1985.
7. Gaiser, G., *Strömungs- und Transportvorgänge in gewellten Strukturen*. Dissertation, Universität Stuttgart, 1990.
8. Holman, J. D., *Experimental Methods for Engineers*, 5th ed. McGraw-Hill, New York, 1989.
9. In Cheol, B. and Soon, H. C., Boiling heat transfer performance and phenomena of Al₂O₃-water nano-fluids from a plain surface in a pool, *International Journal of Heat and Mass Transfer* vol. 48, pp. 2407–2419, 2005.
10. Jorge A. W., Gut, R. F., Pinto, J.M. and Tadini, C. C., Thermal model validation of plate heat exchangers with generalized configurations. *Chemical Engineering Science*, vol. 59, pp. 4591–4600, 2004.
11. Jorge, A. W., Gut, R. F. and Pinto, J. M., Modeling of plate heat exchangers with generalized configurations. *International Journal of Heat and Mass Transfer*, vol. 46, pp. 2571–2585, 2003.
12. Lee, S., Choi, U. S., Li, S. and Eastman, J. A., Measuring thermal conductivity of fluids containing oxide nanoparticles, *ASME J. Heat Transfer*, vol. 121, pp. 280–289, 1999.
13. Martin, H., A theoretical approach to predict the performance of chevron-type plate heat exchangers, *Chemical Engineering and Processing*, vol. 35, pp. 301–310, 1996.
14. Okada, K., Ono, M., Tomimura, T., Okuma, T., Konno, H. and Ohtani, S., Design and heat transfer characteristics of new plate heat exchanger. *Heat Transfer Jpn. Res.* 1, pp. 90–95., 1972.
15. Pak, B. C. and Cho, Y. I., Hydrodynamic and heat transfer study of dispersed fluids with submicron metallic oxide particles. *Exp. Heat Transfer*, vol. 11, no.2, pp. 151-170, 1998.
16. Pantzali, M. N., Mouza, A. A. and Paras, S. V., Investigation the efficiency of nanoluids as coolants in

- Plate Heat Exchangers (PHE), Chemical Engineering Science, vol. 64, pp. 3290 – 3300, 2009.
17. Rosenblad, G. and Kullendorff, A., Estimating heat transfer rates from mass transfer studies on plate heat exchanger surfaces. *Wärme Stoffübertrag*, vol. 8, pp. 187–191, 1975.
 18. Vassallo, P., Kumar, R. and Amico, S. D., Pool boiling heat transfer experiments in silica-water nanofluids, *Int. J. Heat Mass Transfer* vol. 47, pp. 407–411, 2004.
 19. Wright, A. D. and Heggs, P. J., Rating calculation for plate heat exchanger effectiveness and pressure drop using existing performance data. *Trans IChemE*, Vol. 80, Part A, April 2002.
 20. Wang, X., Xian, J., Hai, L., Xin, L., Fang, W., Zhou, F., and Fang, L., Stability of TiO_2 and Al_2O_3 Nanofluids, *CHIN. PHYS. LETT.* Vol. 28, no. 8, 086601, 2011.
 21. Wang, X., Xu, X. and Choi, U.S., Thermal conductivity of nanoparticles-fluid mixture. *J. Thermophys. Heat Transfer* vol. 13, no. 4, pp. 474-480, 1999.
 22. Xuan, Y. and Li, Q., Heat transfer enhancement of nanofluids, *Int. J. Heat Fluid flow*, vol. 21, pp. 58–64, 2000.
 23. Xuan, Y. and Roetzel, W., Conceptions for heat correlation of nanofluids, *Int. J. Heat Mass Transfer*, vol. 43, 3701–3707, 2000.

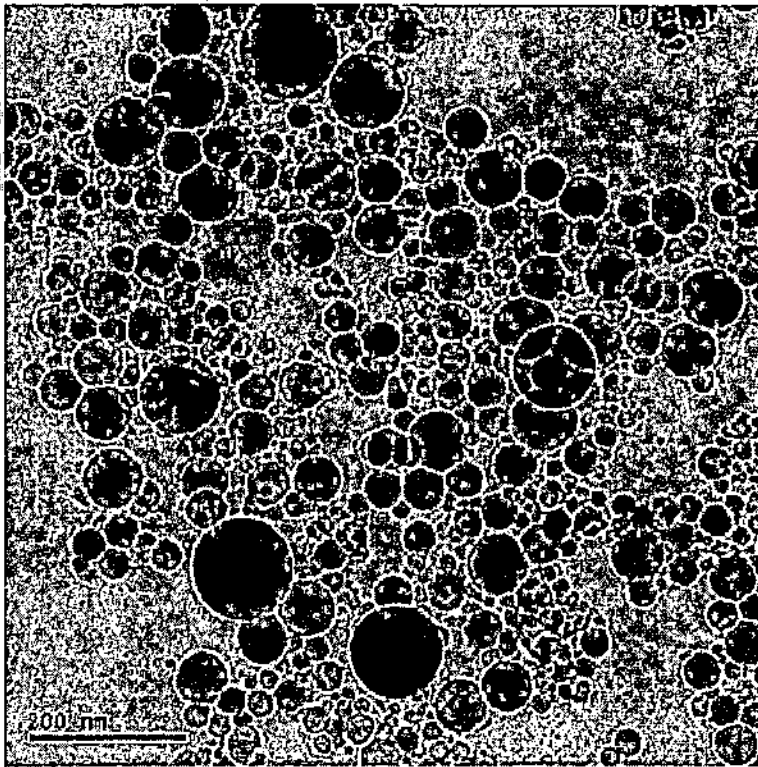


Fig. 1 Characteristics of nano-fluid, TEM photograph of Al₂O₃ nano-particles

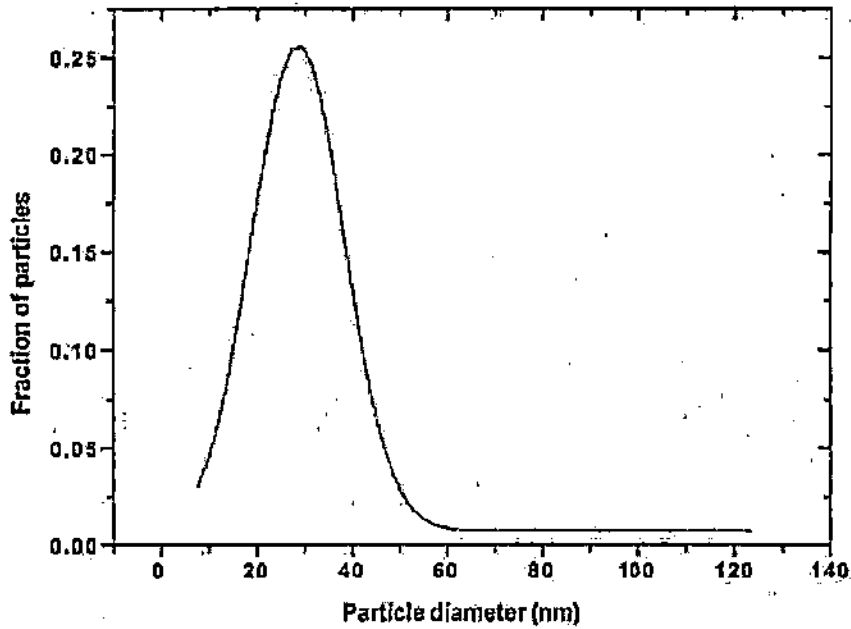


Fig.2 size distribution of the nano-particles

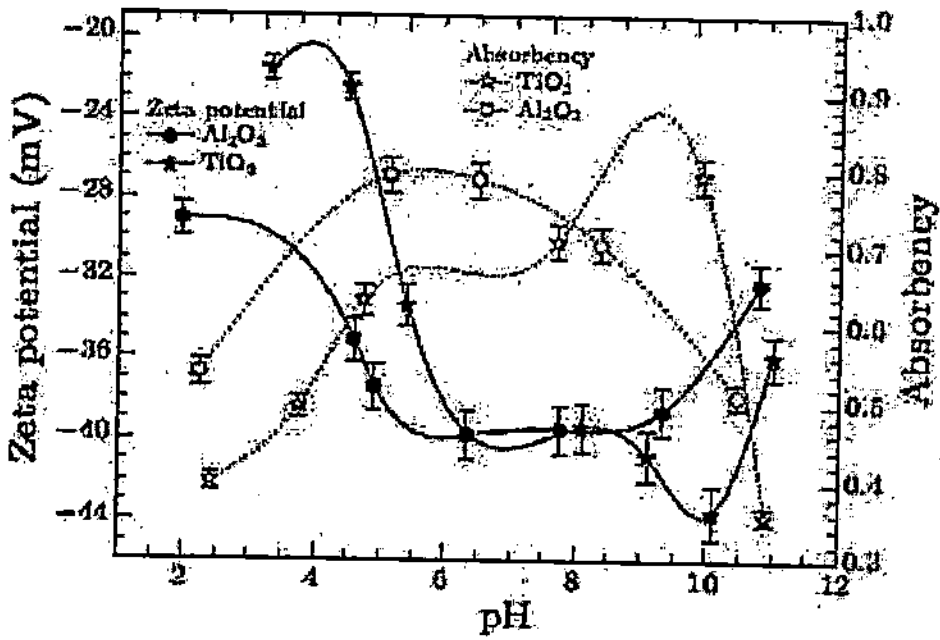


Fig. 3 The changes of zeta potential and absorbency for Al₂O₃- and TiO₂-water nano-fluids as a function of Ph value [20].

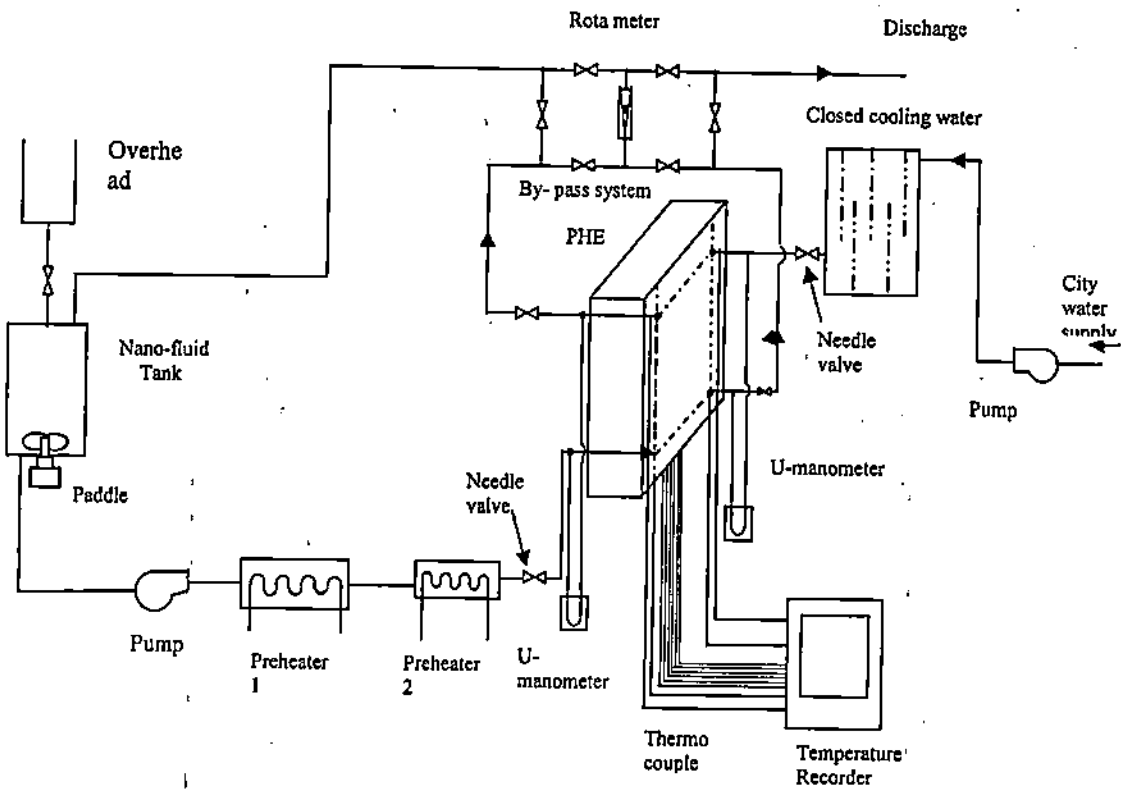


Fig. 4 Experimental Setup

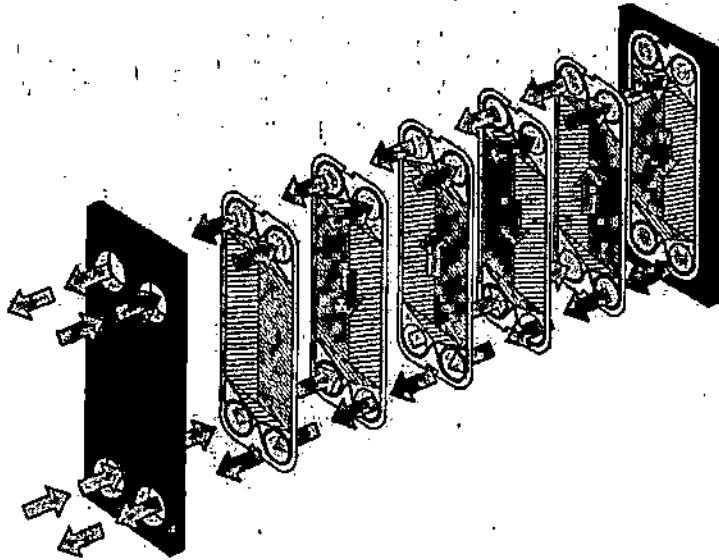


Fig. 5 Flow principal of the plate heat exchanger

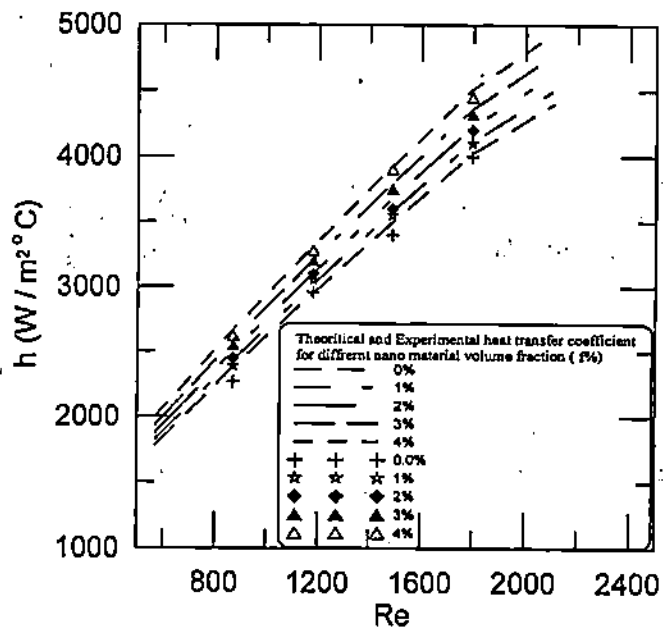


Fig.6 heat transfer coefficient variation with Reynolds number for different Nano material volume fraction

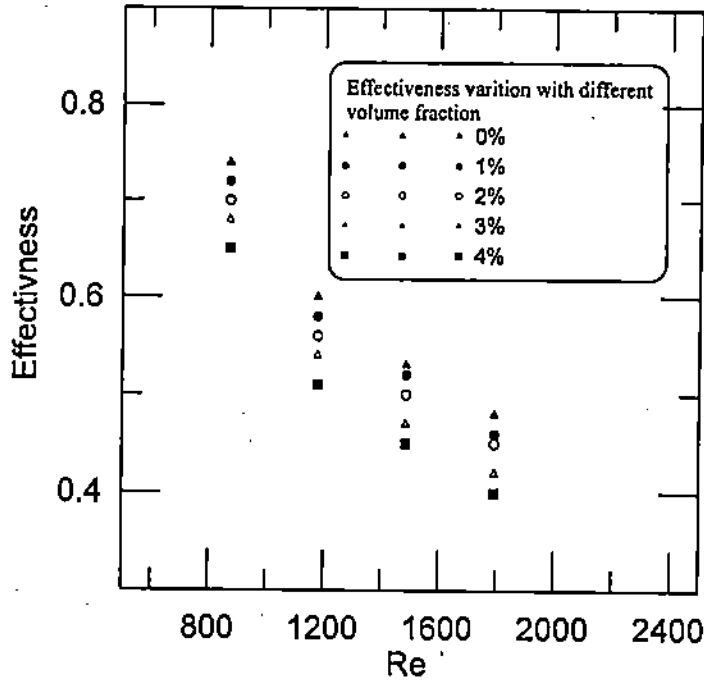


Fig. 7 PHE Effectiveness variation with nano material concentration

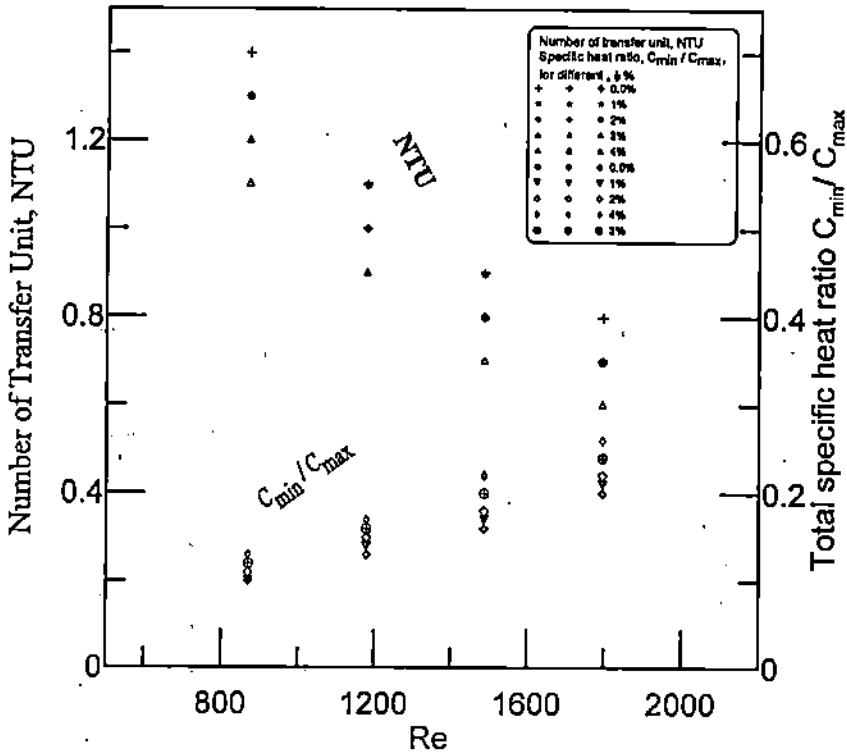


Fig. 8 PHE NTU and specific heat variation

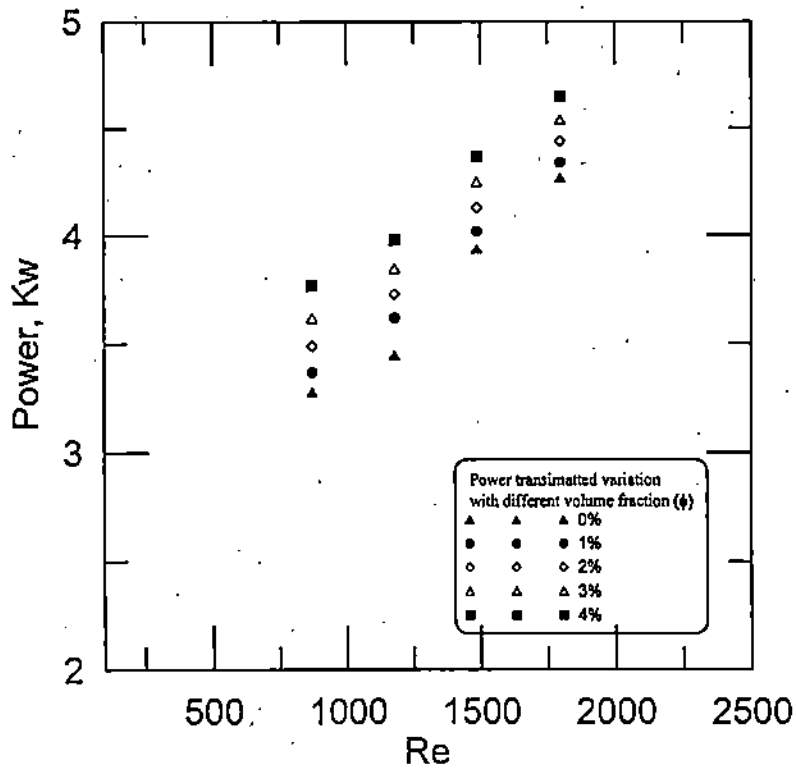


Fig 9 PHE transmitted power

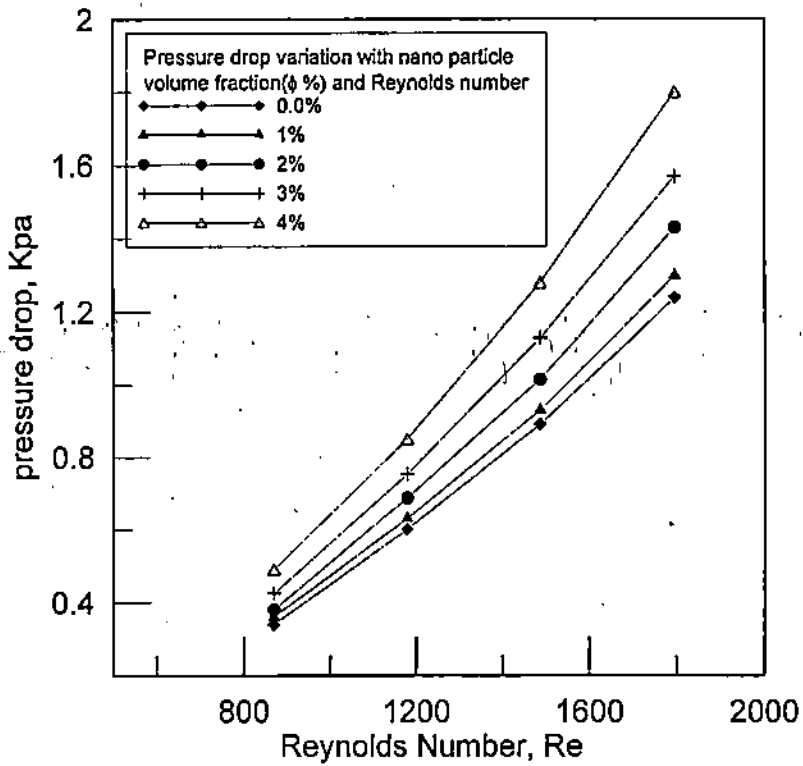


Figure 10 PHE pressure drop variation

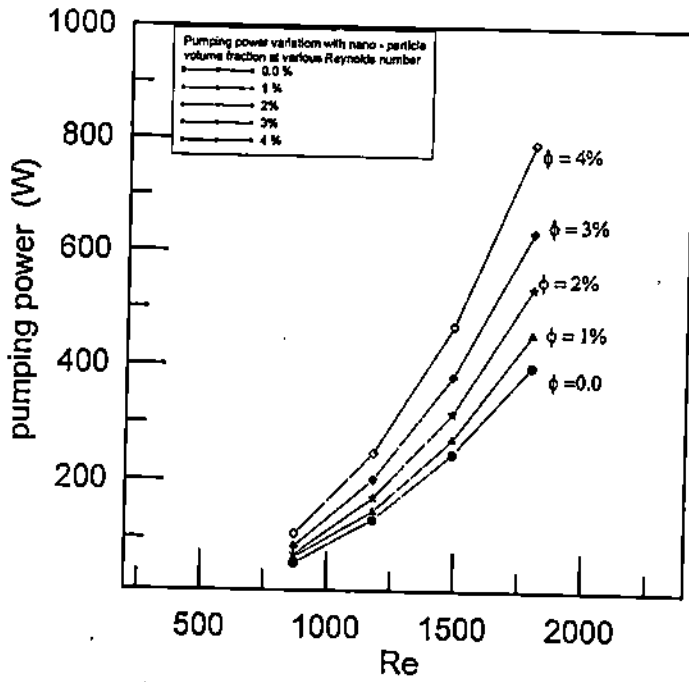


Fig. 11 pumping power variation with Reynolds number and nano- fluid concentration

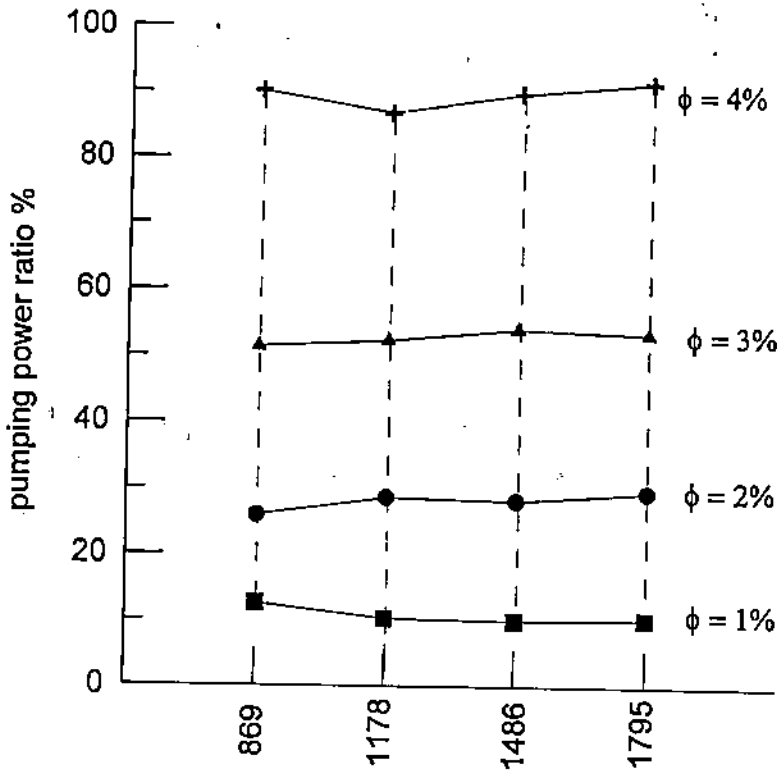


Fig. 12 pumping power ratio relative to cooling water without nano- particle

Table 1. Summary of estimated experimental uncertainties

Primary measurements		Derived quantities	
parameter	uncertainties	parameter	uncertainties
Nano-fluid discharge temperature	3%	Nano-fluid flow rate	5.83%
Hydraulic dia.[3]	0.1	power	6.8%
Plate area	1.2%	Heat transfer coefficient in hot side	9.8%
Nano-fluid density[16]	5%	Nusselt Number	11%
Nano – fluid specific heat [16]	3%	Reynolds Number	7.9%
Nano-fluid viscosity[16]	5%		
Nano-fluid thermal conductivity [16]	5%		

depends on thermo physical properties measurements; hence proper correlations with certain uncertainties are used. The accuracy of measurements and the uncertainties of the derived values are summarized in Table 1. The adopted uncertainty technique is based on that clarified in J.D. Holman [8].

Experimental procedure

The experimental procedure is as follows; both the working fluid and cooling water are circulated by centrifugal pumps. The cooling water loop flow rate is adjusted by using the needle valve and rota meter to a constant fixed flow rate during all the experiments (3.0 m³/hr). A city water supply is used for the cooling process and its temperatures are recorded before and after passing through the PHE. The experiments are carried out at both different nano-fluid Reynolds number and different nano-particles concentration. Each experimental run is executed with its own nano-particle concentration. The nano particles concentration at each run are 0.0 vol%, 1 vol%, 2 vol%, 3 vol% and 4.0 vol% . At each experimental step, the nano-fluid Reynolds number is increased by using the needle valve and the rota meter bypass system. All the experiments are carried out in the laminar flow regime, $Re \leq 2000$. The heating power for the nanofluid is controlled by adjusting the heaters supplied voltage to obtain a constant nano-fluid inlet temperature to the PHE (40 °C) at all the Reynolds number range. The PHE pressure drop variation is measured by U-tube manometer at each variation in nano-fluid Reynolds number.

Theoretical model

A theoretical model was developed before [1] to characterize the PHE performance. That model was based on H. Martin [13] recommended correlations in the laminar flow regime. The heat transfer coefficient was described by the following correlations [13];

$$Nu = Nu^* Pr^{1/3} \left(\frac{\mu}{\mu_w} \right)^{1/6} \quad (17)$$

Where

$$Re \leq 2000$$

17

$$Nu^* = C_q [\zeta \times Re^2 \times \sin(2\phi)]^n \quad (18)$$

The correlations that describe the nano-fluid physical properties (Equ. (1) to Equ. (5)) are linked to this model to generate the theoretical heat transfer coefficient and hence the PHE performance. This theoretical performance is used to compare with experimental results.

IV. RESULTS AND DISCUSSION

The experimental work has been carried out at five runs. At the first run, no nano-material is added to the pure water while from the second run to the fifth run the nano-material concentration was from 1% vol. to 4% vol. At each experimental run, the Reynolds number is increased by using both the needle valve and the flow meter. The inlet – exit fluids temperatures, the plate surfaces temperatures, the fluids flow rates and pressure drops are measured at each measuring state with the investigation of the thermal balance at both the nano-fluid side and the cooling side. By using the aforementioned correlations the average heat transfer coefficient variation with Reynolds number could be measured on the hot side of the PHE as shown in Figure 6. The